



Porous nanoparticles as delivery system of complex antigens for an effective vaccine against acute and chronic *Toxoplasma gondii* infection



Isabelle Dimier-Poisson^{a, b, *, 1}, Rodolphe Carpentier^{c, d, e, 1}, Thi Thanh Loi N'Guyen^{a, b}, Fatima Dahmani^{c, d, e}, Céline Ducournau^{a, b}, Didier Betbeder^{c, d, e}

^a Université de Tours, UMR1282 Infectiologie et Santé Publique, F-37000 Tours, France

^b INRA, UMR1282 Infectiologie et Santé Publique, F-37380 Nouzilly, France

^c Inserm, LIRIC – UMR 995, F-59000 Lille, France

^d Univ Lille, LIRIC – UMR 995, F-59000 Lille, France

^e CHRU de Lille, LIRIC – UMR 995, F-59000 Lille, France

ARTICLE INFO

Article history:

Received 23 October 2014

Accepted 20 January 2015

Available online 19 February 2015

Keywords:

Vaccine

Toxoplasma gondii

Nanoparticles

Nasal immunization

Immunotherapy

ABSTRACT

Development of sub-unit mucosal vaccines requires the use of specific delivery systems or immunomodulators such as adjuvants to improve antigen immunogenicity. Nasal route for vaccine delivery by nanoparticles has attracted much interest but mechanisms triggering effective mucosal and systemic immune response are still poorly understood. Here we study the loading of porous nanoparticles (DGNP) with a total extract of *Toxoplasma gondii* antigens (TE), the delivery of TE by DGNP into airway epithelial, macrophage and dendritic cells, and the subsequent cellular activation. *In vitro*, DGNP are able to load complex antigens in a stable and quantitative manner. The outstanding amount of antigen association by DGNP is used to deliver TE in airway mucosa cells to induce a cellular maturation with an increased secretion of pro-inflammatory cytokines. Evaluation of nasal vaccine efficiency is performed *in vivo* on acute and chronic toxoplasmosis mouse models. A specific Th1/Th17 response is observed *in vivo* after vaccination with DGNP/TE. This is associated with high protection against toxoplasmosis regarding survival and parasite burden, correlated with an increased delivery of antigens by DGNP in airway mucosa cells. This study provides evidence of the potential of DGNP for the development of new vaccines against a range of pathogens.

© 2015 Elsevier Ltd. All rights reserved.

1. Introduction

Vaccines are routinely used to protect human beings against pathogens. They generally contain agents that mimic disease-causing microorganisms and are often made from weakened or killed forms of the target microbe, its toxins or one of its surface proteins. However their use raises several safety issues since pathogenic bioactive material can remain in vaccine formulations as contaminants (LPS, toxins ...). Moreover, to maintain the efficacy of live pathogens, strict storage conditions must be adhered to in order to avoid instability and degradation, and a reversion or a reassortment of the attenuated pathogens with a wild-type,

perhaps leading to the emergence of an infection-bearing vaccine, cannot be discounted [1].

To overcome these issues, subunit vaccines composed of non-living or split pathogens are being developed [2]. However these require adjuvants to increase antigen immunogenicity. For this purpose, nanoparticles are interesting adjuvants that also serve as carriers for the targeted delivery of antigens to immune competent cells [3]. Indeed, formulating protein antigens in nanoparticles has emerged as one of the most promising strategies to trigger an immune response to vaccine antigens [4–8]. Their size, mimicking that of natural pathogens, permits internalization and presentation of antigens by cells and may provoke better recognition by the immune system compared with soluble antigens. Most pathogens infect organisms through a mucosal barrier, and a mucosal delivery system for antigens therefore seems a logical route to investigate.

Toxoplasma gondii, an intracellular protozoan parasite, is the causative agent of toxoplasmosis. It is able to infect all warm-

* Corresponding author. Université de Tours, UMR1282 Infectiologie et Santé Publique, F-37000 Tours, France.

E-mail address: dimier@univ-tours.fr (I. Dimier-Poisson).

¹ Equal contribution.

blooded animals, including humans with a prevalence of between 30 and 70% of the world population, depending on the region [9,10]. Moreover, in animals, toxoplasmosis causes important losses owing to abortions in sheep, which livestock then constitutes a parasitic source for human infection [11]. Mostly, toxoplasmosis is asymptomatic in immune-competent hosts; however it can exhibit severe or fatal symptoms in immune-suppressed hosts because of cerebral cysts reactivation. Another fatal pathology is transplacental infection of fetuses leading to neonatal malformations, ocular diseases or abortions [12]. There is currently no licensed vaccine available for humans.

The natural site of infection by *T. gondii* is the mucosal surface of the intestine. During primary acute infection, *T. gondii* induce a protective mucosal and systemic immunity, which is thought to mainly involve a Th1 cellular immune response focused on IL-12 secreted by dendritic cells (DCs) and interferon-gamma production by CD4+ and CD8+ T lymphocytes [13–20]. Natural infection is particularly interesting as it induces long term protective immunity and highlights the importance of stimulating the mucosal route to immunity in the development of new vaccine strategies against toxoplasmosis. Mucosally delivered vaccines must also, of course, succeed in stimulating cellular immunity, the main mechanism of protection being the establishment of cellular systemic immunity through IFN- γ induction [21,22].

Many studies have shown that partial immunity can be induced after immunization with some *T. gondii* antigens [23–25]. Some mucosal immunization routes have been explored, but the nasal route is an attractive one to induce mucosal and systemic responses to antigens [26]. Cholera toxin is often used as a mucosal adjuvant [27–29]; however safety considerations preclude the use of this adjuvant in vaccine strategies.

Nanoparticles (NP) have been shown to modulate cellular and humoral immune responses [30]. Many types of nanoparticles have been tested [3,31–33], however little is known about the mechanisms by which they trigger an immune response after mucosal administration. We recently developed nanoparticles able to deliver proteins within airway epithelial cells [34]. These nanoparticles can be loaded with proteins and are able to deliver proteins into target cells [35].

In the work presented here, we present the rational design of a nanoparticulate vaccine. We examined the ability of these nanoparticles to be loaded with a total extract of *T. gondii* antigens (TE) both in terms of the percentage of antigen loading and their ability to deliver the antigens via the airway mucosa, macrophages and dendritic cells and to activate these cells. *In vivo* studies of an optimized nanoparticle/antigens formulation after nasal vaccination were performed in acute and chronic models of *T. gondii* infection. Thus, our findings clearly indicate that a nanoparticle-based immunization with complex and heterogeneous proteins is a promising approach to improve vaccination.

2. Materials and methods

2.1. Cell culture and reagents

Maltodextrin was purchased from Roquette (Roquette, France) and DPPG (1,2-dipalmitoyl-sn-glycero-3-phosphatidylglycerol) from Lipoid (Germany). Epichlorohydrin (1-chloro-2,3-epoxypropane), glycidyl-trimethyl-ammonium chloride (GTMA), glacial acetic acid, paraformaldehyde (PFA), 5-[4,6-dichlorotriazin-2-yl] amino-fluorescein (FITC) and Bovine Serum albumin (BSA) were purchased from Sigma Aldrich. Dulbecco-modified essential medium (DMEM), PBS, Fetal Calf Serum (FCS), penicillin/streptomycin antibiotics mixture, L-glutamine and Hoescht 33342 were purchased from Life Technologies. The human bronchial epithelial cell line 16HBE14o- (16HBE) was a kind gift from Pr Dieter Gruenert (University of Vermont, VT, USA).

16HBE cells were maintained in DMEM supplemented with 10% heat-inactivated FCS, 100 U/mL Penicillin, 100 mg/mL streptomycin and 1% L-glutamine at 37 °C in a humidified 5% CO₂ atmosphere. For 8-well glass chamber slides (Lab-TekII, Thermo Scientific Nunc Lab), cells were seeded 3 days before the experiment

at a density of 2.5×10^5 cells per well (0.8 cm²). For 6-well plates, cells were seeded 3 days before the experiment at a density of 1×10^6 cells per well (9.5 cm²).

The THP-1 cells were maintained in high-glucose RPMI supplemented with 10% heat-inactivated FCS, 100 U/mL Penicillin, 100 mg/mL streptomycin, 1 mM sodium pyruvate, 10 mM HEPES, 50 μ M 2-mercapto-ethanol and 1% L-glutamine at 37 °C in a humidified 5% CO₂ atmosphere. For 8-well glass chamber slides (LabTekII, Thermo Scientific Nunc Lab), cells were seeded at a density of 2.5×10^5 cells per well (0.8 cm²) with 20 ng/mL of PMA to induce macrophage differentiation and cell attachment. For 6-well plates, cells were at a density of 1×10^6 cells per well (9.5 cm²) with PMA.

Human foreskin fibroblast (HFF) cells (Hs27 American Type Culture Collection CRL-1634) were cultured at 37 °C in DMEM with 4 mM L-glutamine (Dutscher) supplemented with 10% heat-inactivated Fetal Calf Serum (FCS) (Dutscher) and Hepes 10 mM (Dutscher), in a 5% CO₂ atmosphere.

2.2. Parasite and total extract (TE) preparation

Two strains of *T. gondii* (RH and 76 K) were used in this study. Cysts of the 76K strain (Type II) were obtained from the brain of orally infected CBA/J mice and maintained by monthly passage. The tachyzoites of the RH strain (Type I) were obtained by passage in HFF cells and used to prepare the total *T. gondii* antigen extract (TE) as previously described [36]. About $3 \cdot 10^8$ tachyzoites were obtained from one 225 cm² culture flask corresponding to 1 mg of TE. Lysis of tachyzoites were performed by freeze/thaw cycles, pooled, sonicated and centrifuged. The protein content of the supernatant (TE) was evaluated by micro BCA method.

2.3. DGNP synthesis

Porous maltodextrin-based with lipid core nanoparticles (DGNP) were prepared as described previously [37]. Briefly, maltodextrin were dissolved in 2 N sodium hydroxide with magnetic stirring at room temperature. Addition of epichlorohydrin and GTMA yielded a cationic polysaccharide gel that was then neutralized with acetic acid and crushed using a high pressure homogenizer (Emulsiflex C3, France). The nanoparticles thus obtained were purified by tangential flow ultra-filtration (Centramate Minim II, PALL, France) using a 300 kDa membrane (PALL, France) and mixed with DPPG above the gel-to-liquid phase transition temperature to produce DGNP.

2.4. Size and zeta potential measurements

The average diameter of DGNP was measured by dynamic light scattering in 15 mM NaCl and the zeta potential was measured by photon correlation spectroscopy in pure water using a zetasizer nanoZS (Malvern Instruments, France). Measurements were carried out in triplicate.

2.5. Transmission electron microscopy characterization

Micrographs were taken with a low-voltage (5 kV) transmission electron microscope LVEM5-TEM (DeLong Instrument, Brno, Czech Republic) and obtained by Dr Benoit Maxit (Cordouan Technologies, France). Samples were prepared by placing 5 μ L (5 mg/mL) of DGNP on 300 mesh ultrathin carbon film copper grids (Cu300-HD from Pacific Grid Tech, San Francisco, United States). After removal of the excess of water using a filter paper, the TEM grids were air-dried at room temperature for 10 min prior to analysis.

2.6. Protein labeling and DGNP loading

Both BSA and TE were labeled with FITC according to previously described protocol [16]. Briefly, 1 mg of FITC was added to 10 mg of proteins (mass ratio of 10) solubilized in 0.1 M bicarbonate buffer (pH 9.5), and the solution was mixed for 6 h in the dark at room temperature. The preparation was filtered by gel filtration on a PD-10 Sephadex desalting column (Sigma–Aldrich). Loading of DGNP with FITC-labeled proteins were done by mixing both components at room temperature for 30 min.

2.7. Loading of proteins into DGNP

T. gondii antigens were formulated with DGNP in water. Different mass ratios of DGNP (30 μ L) were mixed with 15 μ L of the antigen suspension for 30 min at room temperature. Formulations were supplemented with a non denaturing buffer (Tris–HCl 125 mM (pH 6.8), 10% glycerol, 0.06% bromophenol blue) for native electrophoresis, or a denaturing buffer (Tris–HCl 125 mM (pH 6.8), 20% glycerol, 10% SDS, 2.5% b-mercaptoethanol and 0.06% bromophenol blue) for SDS-PAGE. Samples were analyzed by polyacrylamide gel electrophoresis (PAGE), using a 10% acrylamide-bisacrylamide gels stained by the silver nitrate method.

2.8. Cellular delivery of proteins by DGNP

16HBE cells were plated for 3 days in 6-well plates for flow cytometry or in 8-chamber slides for confocal microscopy. After three washes with PBS, cells were treated for 15 or 60 min with DGNP loaded with FITC-labeled proteins and washed again with PBS. For flow cytometry, cells were detached with trypsin, harvested by centrifugation and diluted in PBS before analysis on a CyAn ADP Analyzer (Beckman Coulter). Cells were selected by their size and cellular complexity (SSC and FSC). For

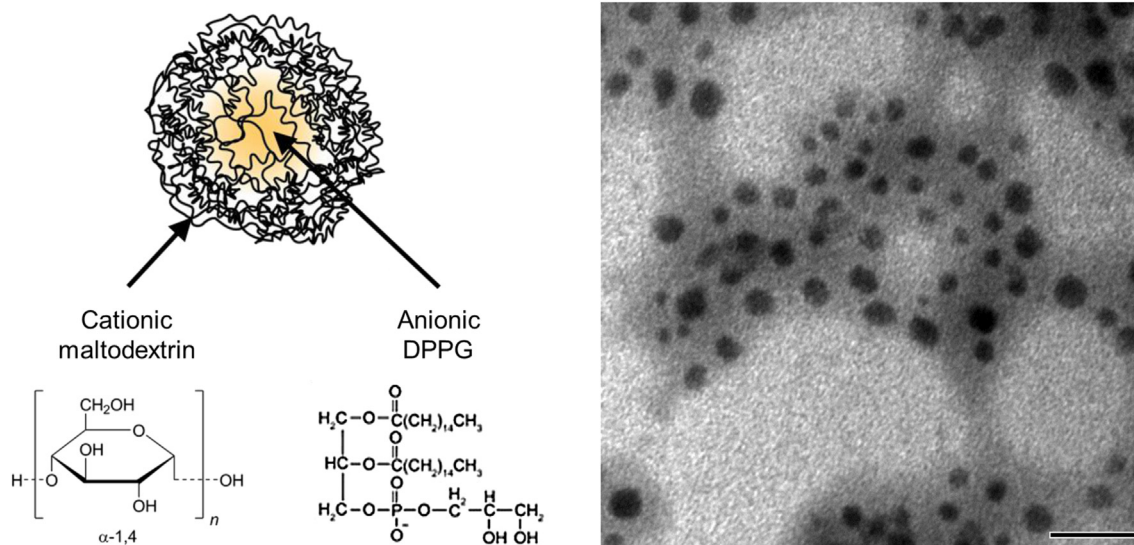


Fig. 1. Representation of DGNP nanoparticles. (Left) Schematic representation of DGNP nanoparticles showing chemical structure of maltodextrin and DPPG. (Right) Transmission electronic microscopy of nanoparticles. Nanoparticles were prepared in water and processed for benchtop electronic microscopy as described in the methods section. Result shows a representative TEM image. Scale Bar: 100 nm.

each event, fluorescence intensities (FITC) were reported. The percentage of cells over the background (untreated cells) and the mean fluorescence intensities were expressed, thus measuring the percentage of cells with intracellular FITC-labeled proteins and the level of the fluorescence, respectively. For confocal microscopy, cells were fixed for 10 min with 4% (vol:vol) paraformaldehyde at 4 °C and nuclei were stained with Hoescht 33342.

2.9. *In vitro* evaluation of NF-κB pathway activation and TLR screening

The THP-1Blue™ NF-κB cells (Invivogen) were derived from the human THP-1 monocyte cell line by stable integration of an NF-κB-inducible secreted embryonic alkaline phosphatase (SEAP) reporter construct, and respond only to ligands for TLR2, TLR1/2, TLR2/6, TLR4, TLR5 and TLR8. Cells were grown in RPMI 1640 supplemented with 2 mM L-glutamine, 1.5 g/L sodium bicarbonate, 4.5 g/L glucose, 10 mM Hepes, 1 mM sodium pyruvate, penicillin/streptomycin (50 U/mL–50 μg/mL) and 10% heat-inactivated FCS. The THP-1Blue™ NF-κB cells were cultured in triplicate, $1 \cdot 10^5$ cells in 96-well plates were seeded under different stimulation conditions in 200 μL for 18 h: cells alone, poly(I:C) 2.5 μg/mL, LPS 2.5 ng/mL, DGNP 20 μg/mL, TE 2 μg/mL or DGNP/TE (20 μg/mL DGNP and 2 μg/mL TE). After incubation, 20 μL of each supernatant was added to 180 μL of Quanti-Blue™ (Invivogen) and the SEAP level was determined with an Absorbance Microplate Reader (BioHit) at 630 nm.

Screening for TLR ligands was performed by Invivogen using a panel of HEK293-TLR-Blue clones, engineered to express only a single specific TLR, and a SEAP–reporter plasmid activated with NF-κB transcription factor. Cells incubated with TLR-specific ligands were used as a positive control: DGNP were tested at 20 μg/mL, TE at 2 μg/mL and DGNP/TE (20 μg/mL DGNP and 2 μg/mL TE) and TLR activation was evaluated as an increase in SEAP activity measured as absorbance at OD650 nm, using Quanti-Blue reagent (InvivoGen).

2.10. Mice

Female 6–8 weeks-old CBA/J (H-2k) mice were purchased from CER Janvier (Le Genest Saint Isle, France) and maintained under pathogen-free conditions in our

animal house. Experiments were carried out in accordance with the guideline for animal experimentation (EU Directive 2010/63/EU) and the protocol was approved by the local ethics committee at Tours University (CEEA VdL).

2.11. *In vitro* maturation of bone marrow DC and peritoneal MØ, and cytokine secretion measurements

Bone marrow cells were collected from femurs and tibias of 6–8 weeks old CBA/J mice and cultured in RPMI 1640 with glutamine supplemented with 10% heat-inactivated FCS, 15 mM Hepes, 50 μM 2-β-mercaptoethanol, 100 U/mL penicillin/Streptomycin, 1% Pyruvate and 1% non essential amino-acids at 37 °C, in a 5% CO₂ atmosphere. Differentiation of Bone Marrow Dendritic cells (BMDC) was obtained by adding 20 ng/mL of GM-CSF from J558 cells line supernatant. BMDC were harvested after 8 days of culture.

Primary mouse macrophages were obtained from CBA/J mice by peritoneal lavage. Murine peritoneal macrophages were cultured in 6-well tissue culture plates (4×10^6 cells/well) and maintained in RPMI medium supplemented with antibiotics and 10% FCS at 37 °C in 5% CO₂ for 4 h.

DGNP, free TE or DGNP-encapsulated TE (diluted in the cell culture medium at 5 μg/mL), were added to 1 million differentiated BMDCs and MØ and incubated for 24 h at 37 °C in 5% CO₂. Cell culture supernatants were collected after 24 h and stored at –20 °C for further cytokine quantification. Cytokine productions were evaluated using commercial ELISA kits according to the manufacturer's instructions (e-Bioscience, San Diego, CA, USA, except for IL-12 p40 from DuoSet, R&D Systems, Minneapolis, MN, USA).

2.12. Intranasal immunization and challenge

The CBA/J mice received three doses intra-nasally at 2-week intervals of 30 μg DGNP, 10 μg free TE, 1 μg of CT, 10 μg TE in association with 1 μg of CT (Sigma) and 10 μg TE loaded in 30 μg DGNP (DGNP/TE) (6 μL per nostril).

One month after the final immunization, mice (10 per group) were infected orally with 120 cysts (lethal dose) or 30 cysts (sub-lethal dose) of the 76K strain. Six weeks after the challenge, the mice were killed and their brains removed. Each brain was homogenized in 5 mL of RPMI medium and the number of cysts per brain was determined microscopically by counting eight 10 μL samples of each homogenate.

2.13. Humoral response

Measurement of IgG and IgG subclass response was performed on blood collected by sub-mandibular puncture before vaccination and at intervals afterwards. Samples were tested by ELISA using TE at 10 μg/mL. Limited dilutions of serum samples in PBS-T20 were added and bound antibodies were detected with alkaline phosphatase-conjugated anti-mouse IgG (Sigma–Aldrich) diluted 1/5000, or HRP-conjugated anti-mouse IgG1 or IgG2a (BD Biosciences) at 1/1000 in PBS-T20. Presence of IgG or IgG1/IgG2a was detected by p-nitro-phenyl-phosphate at 405 nm and TMB substrate (Sigma–Aldrich) at 450 nm respectively with Absorbance Microplate Reader (BioHit). The mice from the control group were used as a negative control.

Table 1

Size and zeta potential of nanoparticles (DGNP), antigens (BSA or TE) and antigen-loaded nanoparticles (DGNP/BSA or DGNP/TE). DGNP were mixed with BSA or TE for 30 min at a ratio of DGNP/Proteins (3:1, w:w). Size and Zeta potential are measured in triplicate by dynamic light scattering on a Zetasizer NanoZS. pdi: polydispersity index.

	Size (nm)	pdi	Zeta potential (mV)
DGNP	71.2	0.155	+38.3 ± 5.7
BSA	4.7	0.189	–58.3 ± 10.4
DGNP/BSA	88.7	0.230	+34.1 ± 5.4
TE	482.4	0.458	–33.5 ± 6.0
DGNP/TE	88.4	0.512	+37.4 ± 7.0

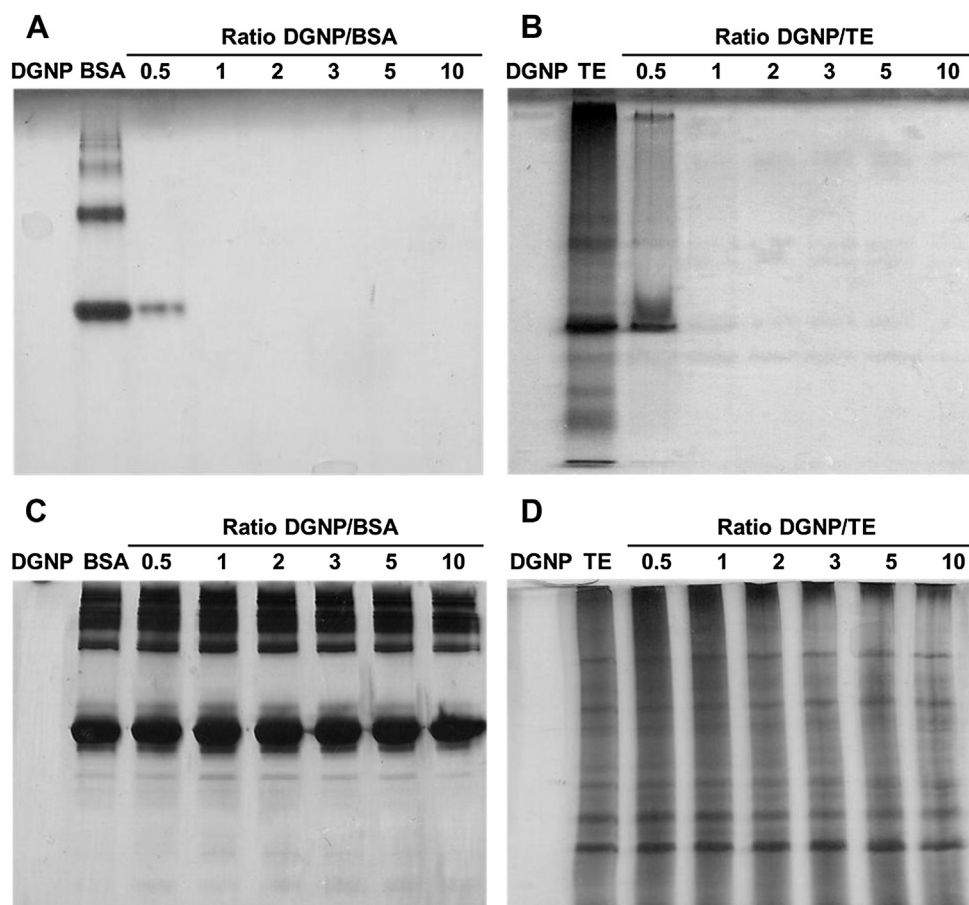


Fig. 2. Polyacrylamide gel electrophoresis (PAGE) analysis of nanoparticle-protein interactions. DGNP (from 2 to 40 μg) were mixed with 4 μg of BSA (A) or TE (B) for 30 min at different mass ratios. The formulations were loaded onto native polyacrylamide gels for non-denaturing electrophoresis and gels were stained by the silver nitrate method. Control DGNP lane was loaded with the maximum amount corresponding to 40 μg . From a mass ratio of 1:1 (DGNP/proteins), unbound proteins were not detectable meaning that loading of the proteins within DGNP was complete. To release proteins from DGNP, SDS-PAGE was performed with BSA (C) or TE (D) under similar conditions to (A) and (B), respectively. Silver nitrate staining showed that proteins were loaded to DGNP before denaturing electrophoresis.

2.14. Cellular response

Mice were sacrificed one month after the last immunization. Spleen and mesenteric lymph nodes (MLN) were harvested under sterile conditions.

Spleens and MLN were dissociated into single-cell suspensions with gentle-MACS™ (Miltenyi Biotec). Hypotonic shock (0.155 M NH_4Cl , pH 7, 4) was used to remove splenic erythrocytes. The cells were then suspended in RPMI 1640 (Dutscher) supplemented with 5% FCS, HEPES (25 mM, Dutscher), L-glutamine (1 mM, Dutscher), sodium pyruvate (1 mM, Dutscher), β -mercaptoethanol (50 μM), and penicillin-streptomycin (1 mM, Dutscher).

For cytokine assays, 6 mice per group were dedicated to the study of cellular response by Cytometric Bead Array Th1/Th2/Th17 (BD Biosciences): $5 \cdot 10^5$ cells were cultured in flat-bottomed 96-well cultures plates in 100 μL of culture medium alone or with 10 $\mu\text{g}/\text{mL}$ of TE or 10 $\mu\text{g}/\text{mL}$ of concanavalin A as a positive control of proliferation. The plates were incubated for 2 days at 37 °C in 5% CO_2 and harvested supernatants from restimulated splenocytes and MLN cells were analyzed using Th1/Th2/Th17 cytometric bead array for IFN- γ , TNF- α , IL-2, IL-4, IL-6, IL-10 and IL-17A.

For Elispot assays (performed using MABTECH Mouse IFN- γ Elispot Plus kit/ALP), $5 \cdot 10^5$ and $1 \cdot 10^6$ cells were seeded alone or with stimulatory agents (10 $\mu\text{g}/\text{mL}$ of TE or 10 $\mu\text{g}/\text{mL}$ of Concanavalin A) into precoated 96-well plates for 48 h at 37 °C in a humidified incubator with 5% CO_2 . Spots were detected by 1 $\mu\text{g}/\text{mL}$ of detection antibody/biotin and then by Streptavidin/ALP. Revelation was performed by BCIP/NBT and spots were counted in ELISpot reader (Biosys®, Bioreader 5000).

Involvement of CD4+ or CD8+ T cells in the secretion of cytokines was studied by incubating $5 \cdot 10^5$ splenocytes (in triplicate) in flat-bottomed 96-well plate for 72 h. Cells were cultured alone or in the presence of stimulatory agents (20 $\mu\text{g}/\text{mL}$ of TE or 10 $\mu\text{g}/\text{mL}$ of Concanavalin A) and in the presence or absence of 20 $\mu\text{g}/\text{mL}$ anti-CD4 mAb or anti-CD8 mAb (eBiosciences) at 37 °C in a humidified incubator with 5% CO_2 . After 72 h, supernatants of restimulated splenocytes were harvested and cytokines (IFN- γ and IL-17A) were assayed using eBiosciences ELISA kit Set Mouse.

2.15. Statistical analysis

One-way ANOVA and Two-way ANOVA plus post-test were used to determine the significance of variations between groups using GraphPad Prism software.

3. Results

3.1. DGNP characterization

DGNP are porous nanoparticles (NPs) prepared from maltodextrin as previously described [37] with anionic phospholipids in their core (Fig. 1). The nanoparticles have a mean diameter of 71.2 nm and a pdi of 0.155 (Table 1). Their size was confirmed by TEM and DGNP were found to be almost spherical (Fig. 1).

3.2. Loading of DGNP with proteins

Owing to the complexity of *Toxoplasma* antigens, we focused first on the association of the NPs with a purified protein. BSA was loaded by mixing premade nanoparticles and proteins at room temperature [37]. To test the loading capacity of DGNP, various amounts of nanoparticles (from 2 μg to 40 μg) were mixed with 4 μg of BSA and the resulting formulations (DGNP/BSA mass ratio from 0.5 to 10) were analyzed by polyacrylamide gel electrophoresis under non-denaturing conditions (native PAGE) to allow the electrophoretic migration of unbound proteins from the

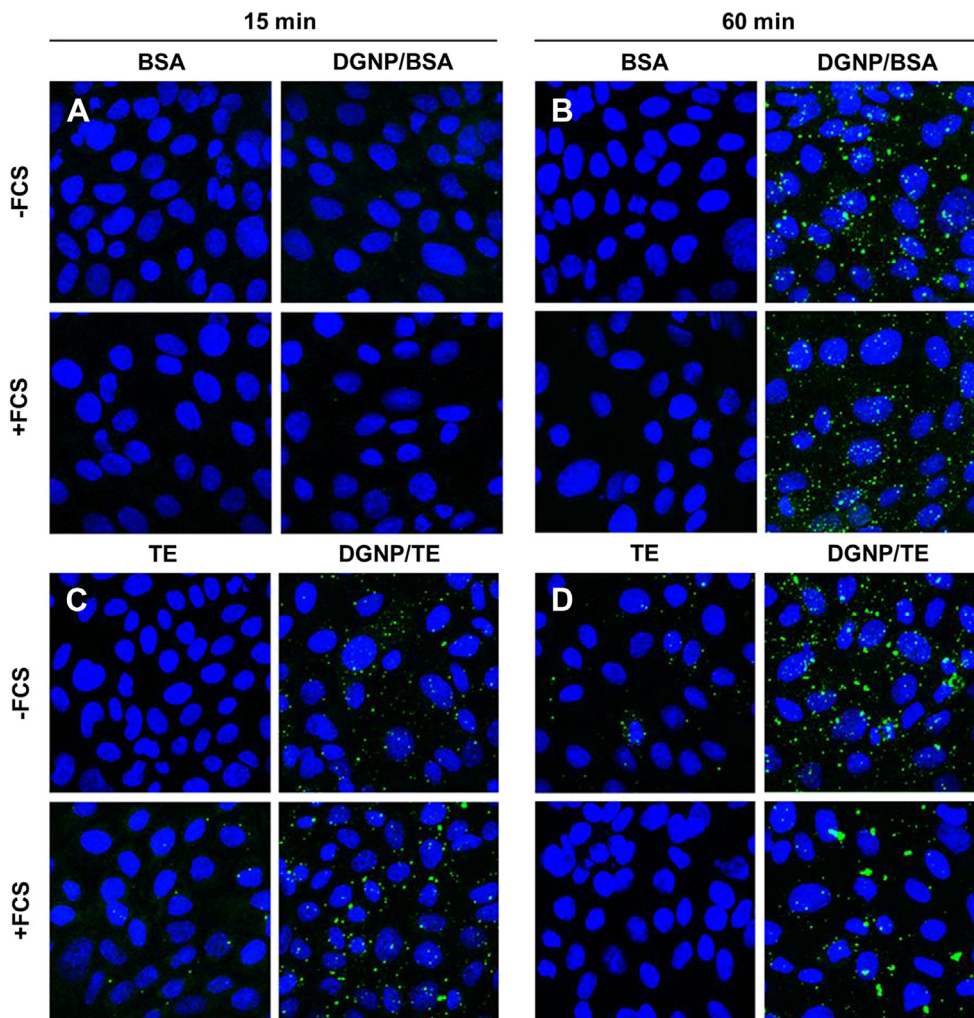


Fig. 3. Confocal analysis of the delivery of proteins into epithelial cells by nanoparticles. 16HBE cells were treated with free or DGNP-formulated BSA (DGNP/BSA, 3:1 w:w) for 15 (A) or 60 min (B) with or without 10% FCS; BSA and TE were labeled with FITC (green). Cells were then washed, fixed in PFA and nuclei were stained with Hoechst (blue). Slides were mounted with Fluoroshield and observed by confocal microscopy with an original magnification of $\times 40$. Representative pictures are shown. Delivery of proteins into epithelial cells was increased under all conditions with DGNP formulations.

formulations. We observed that from a 1:1 ratio of DGNP/BSA (weight:weight), the loading of BSA to NP was stoichiometric (Fig. 2A). This result highlights the fact that the interactions between DGNP and BSA are strong. Electrophoresis performed under denaturing conditions (SDS-PAGE) totally released the protein from NP (Fig. 2C).

Size and zeta analysis of DGNP/BSA formulations confirmed that BSA was completely loaded into the core of the NPs and not adsorbed to NP surfaces. BSA has a mean size of 4.7 nm and a zeta potential of -58.3 mV (Table 1). The size analysis of DGNP/BSA showed only a single population with a mean diameter of 88.7 nm, confirming the complete loading of the proteins into DGNP. Zeta potential analysis showed that BSA was completely inserted in the core of the nanoparticles and not adhered on their surfaces (Table 1).

3.3. Delivery of BSA by DGNP

We evaluated the delivery of proteins to airway epithelial cells using confocal microscopy and flow cytometry. Cells were treated with free BSA or with DGNP/BSA for 15 or 60 min in the presence or absence of 10% fetal calf serum (FCS). Confocal microscopy showed

that after 60 min of treatment, only DGNP effectively delivered BSA into the epithelial cells. Interestingly, serum did not significantly decrease the penetration of BSA into the cells (Fig. 3A–B). To quantify the delivery of proteins into the epithelial cells, flow cytometry analysis were performed. The percentage of cells having endocytosed BSA increased from 54 to 71% when DGNP nanoparticles were used (Fig. 4A). After 15 min, BSA was delivered into the cells by DGNP while uptake of free BSA was not detected (control: 14.97, free BSA: 16.40, DGNP/BSA: 37.41; control with serum: 14.29; free BSA with serum: 13.92, DGNP/BSA with serum: 27.86). After 60 min of treatment, small amounts of free BSA were detected in the cells but this was reduced in the presence of serum (control: 14.62, free BSA: 26.19; control with serum: 14.81; free BSA with serum: 18.46). Interestingly, BSA loaded into DGNP was efficiently delivered to the cells in both the absence and presence of serum (DGNP/BSA serum absent: 87.79; DGNP/BSA serum present: 40.50) (Fig. 4B). Taken together, these results demonstrate that it is possible to load DGNP with BSA and that DGNP act as vectors to effectively deliver BSA into airway epithelial cells. We further wanted to determinate whether DGNP could be loaded with a complex and heterogeneous mixture of antigens for a vaccine application.

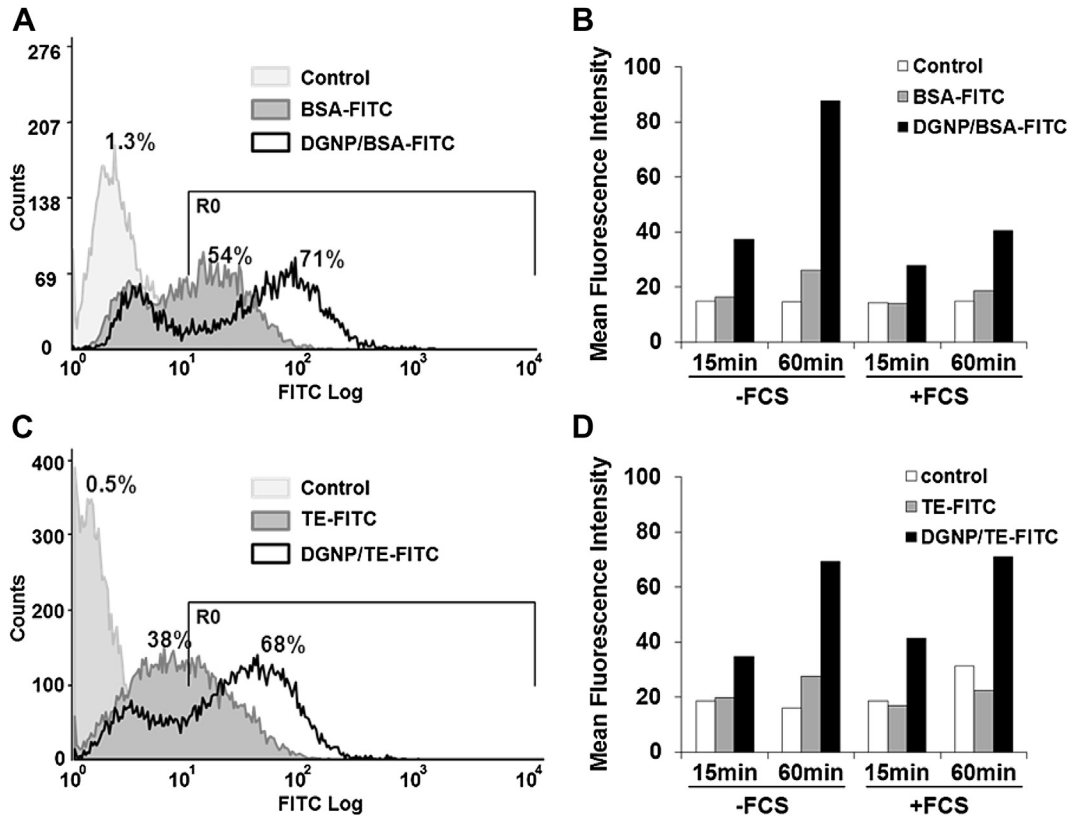


Fig. 4. Flow cytometry analysis of the delivery of proteins into epithelial cells by nanoparticles. 16HBE cells were treated with free or formulated BSA-FITC (DGNP/BSA, 3:1 w:w) for 15 or 60 min, with or without 10% FCS: (A) Representative results of the delivery of BSA after 60 min of treatment without FCS. R0 is set as a gate over the autofluorescence background. Percentages shown are of positive cells in R0. Data were collected on a minimum of 5000 cells on FSC/SSC graph plot (not shown); (B) Overall results of mean fluorescence intensity gated in R0. Formulations of TE under similar conditions to those used for BSA treatments are shown in (C) and (D).

3.4. Loading of DGNP with TE of *T. gondii*

Loading of DGNP with TE was determined by polyacrylamide gel electrophoresis using various DGNP/TE (w:w) ratios. From a DGNP/TE of 1, total loading of DGNP with TE was observed (Fig. 2B). As

observed with BSA, loading appeared stoichiometric since at a DGNP/TE ratio of 0.5 (w:w) full association was not achieved. An SDS-PAGE analysis showed that the proteins can be released from DGNP (Fig. 2D). Taken together, these results suggest that the interactions between DGNP and TE were very stable, despite the

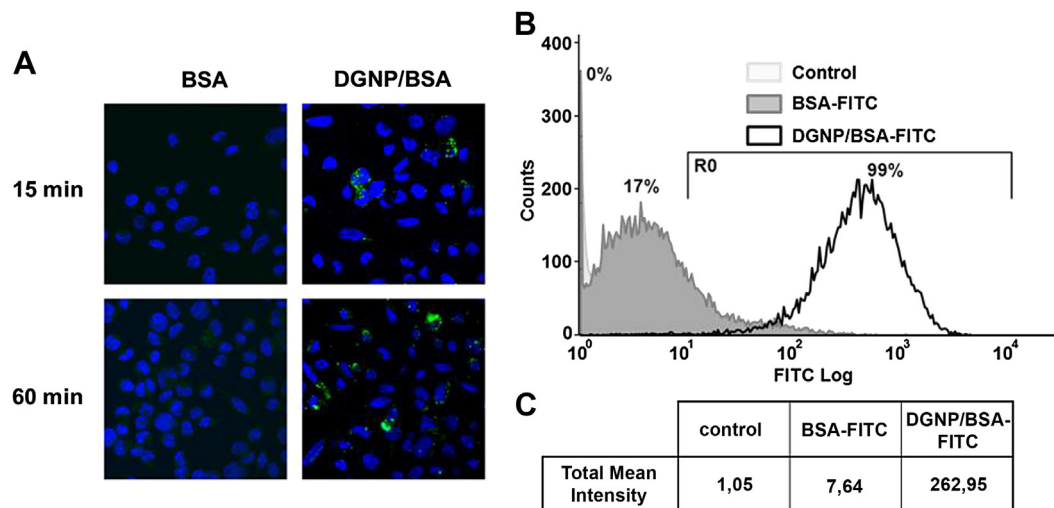


Fig. 5. Analysis of the delivery of proteins by nanoparticles into macrophage cells. The PMA-differentiated THP1 macrophage cells were treated with free or DGNP-encapsulated BSA (DGNP/BSA, 3:1 w:w) for 60 min without FCS. (A) Confocal analysis of the delivery. Cells were washed, fixed in PFA and nuclei were stained with Hoescht (blue). Slides were mounted with Fluoroshield and observed by confocal microscopy with an original magnification of $\times 40$. (B and C) cytometry analysis of BSA delivery. Cells were washed, harvested with trypsin and processed on a Cyan ADP analyzer for cytometry. Data were collected on a minimum of 10,000 cells. R0 is set as a gate over the autofluorescence background. Percentages of positive cells (having incorporated TE) in R0 are given (B). The table represents the mean fluorescence intensities (amount of incorporated TE) in the whole samples extracted from the graph (C). Results show that the delivery of proteins into PMA-differentiated THP1 macrophage cells is increased by nanoparticles.

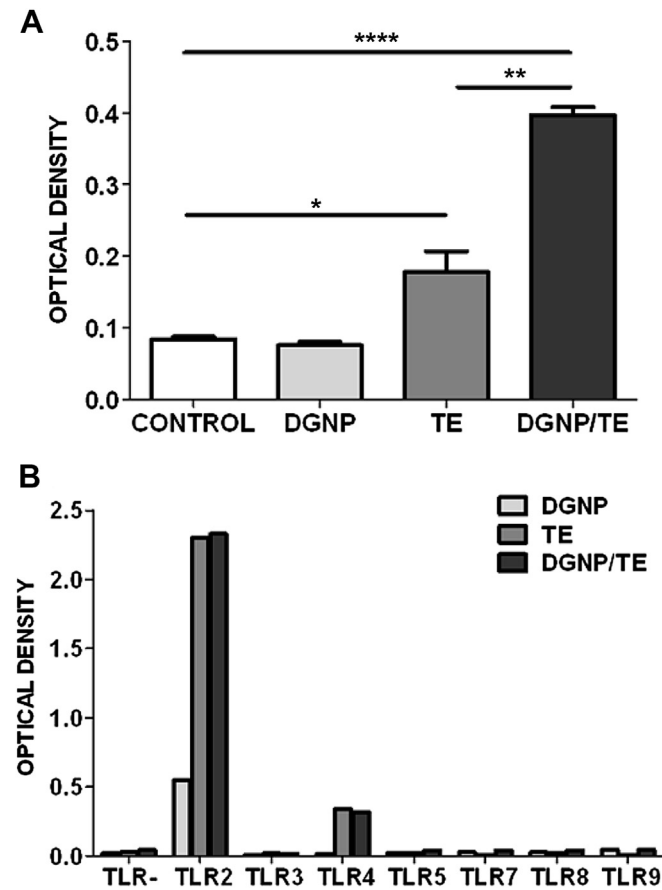


Fig. 6. Investigation of the NF- κ B signal transduction and TLR activation pathways by DGNP, TE and DGNP/TE. (A) Investigation of the NF- κ B signal transduction pathway following DGNP, TE and DGNP/TE treatment of cultured THP1-Blue™ NF- κ B cells. The NF- κ B gene expression was significantly upregulated at 18 h after DGNP/TE treatment. (B) Identification of the TLR pathways involved in the signaling of TE. Responses of the TLR transfected HEK-TLR-Blue cell lines (Invivogen) stimulated with DGNP, TE and DGNP/TE. As a positive control, cells were activated with their respective canonical agonists (data not shown). TE and DGNP/TE acts through TLR2 and TLR4. Data are expressed as the means \pm SEM of duplicate measures of two independent experiments. *: $p < 0.05$; **: $p < 0.01$, ****: $p < 0.0001$.

heterogeneity in molecular weight of the TE proteins. Size and zeta potential analysis of the formulations confirmed that antigens are loaded within the core of DGNP (Table 1) and not merely adsorbed to their surfaces. These results additionally demonstrate the potential of NP vectors to be loaded with a wide variety of proteins.

3.5. Delivery of TE by DGNP into airway mucosa cells

Interestingly, confocal microscopy showed that after 15 min of incubation, free TE did not enter the cells while DGNP favored its delivery (Fig. 3C). After 60 min, only low amounts of proteins were found in the cells treated with free TE, and then only in the absence of serum. On the contrary, DGNP-formulated TE was efficiently delivered into the cells in the absence or presence of serum (Fig. 3D). Furthermore, flow cytometry showed that after 60 min of incubation without serum, an increase in the percentage of cells having endocytosed the protein was observed (from 38% to 68%, respectively, Fig. 4C). After 15 min, TE was delivered into the cells by DGNP while free TE failed to be really detected in the cells (control: 18.46, free TE: 19.82, DGNP/TE: 34.58; control with serum: 18.51; free TE with serum: 16.88, DGNP/TE with serum: 41.22). Only DGNP favored the delivery of TE delivery into the cells, confirming their

utility as an antigen delivery system (control: 16.06, free TE: 27.51, DGNP/TE: 69.14; control with serum: 31.33; free TE with serum: 22.46; DGNP/TE with serum: 71.08). Interestingly, delivery of TE by DGNP did not seem to be influenced by the presence of serum (Fig. 4D).

3.6. Delivery of proteins into immune cells

Epithelial cells constitute the first cellular barrier of the organism, however one cannot preclude that DGNP-formulated antigens could target directly or be transferred indirectly to immune cells. To answer this question, confocal and flow cytometry analysis of the delivery of a protein into PMA-differentiated THP-1 macrophage cells were performed. Macrophages were treated for 15 or 60 min with BSA or DGNP/BSA in the absence of serum. After 15 min incubation, confocal microscopy revealed that free BSA did not enter the macrophage while DGNP was able to deliver the protein, and the amount delivered increased after 60 min incubation (Fig. 5A). Quantitative analysis by flow cytometry confirmed that the percentage of FITC-positive cells and mean fluorescence intensities of intracellular BSA was highly increased by DGNP (Fig. 5B and C). This suggests that DGNP are able to efficiently deliver antigens into macrophages.

The next step was to evaluate the ability of DGNP/TE vaccine formulation to activate immune cells *in vitro*.

3.7. NF- κ B pathway activation by TE encapsulation and identification of the TLR pathways

To characterize DGNP/TE vaccine regarding its biological function, activation of NF- κ B signaling was evaluated on THP1-Blue™ NF- κ B cells. The THP1-Blue cells were incubated with DGNP, TE and DGNP-formulated TE and assayed for NF- κ B-inducible secreted embryonic alkaline phosphatase (SEAP), a reporter of NF- κ B activation. As shown in Fig. 6A, DGNP/TE increased by 2.5 fold the secretion of SEAP compared to TE, and hence NF- κ B activation.

We also evaluated whether TLR were involved through NF- κ B-mediated gene expression. To determine whether DGNP/TE vaccine acts through TLRs, and to precisely identify the TLR pathways activated, their ability to activate TLRs was analyzed in cell-based assays using HEK293-TLR-Blue clones, each expressing a single human TLR2 through TLR9, and a reporter gene (SEAP) under the control of TNF- α . Incubation with free TE or DGNP/TE significantly increased SEAP production only in cells expressing either TLR2 or TLR4 receptors (Fig. 6B). Our results suggest that both TLR2 and TLR4 receptors participate in the induction of the protective immune response against *T. gondii* infection independently of any action induced by the nanoparticles.

3.8. Immuno-stimulatory efficiency of DGNP/TE vaccine on dendritic cells and macrophages

The activation of APCs is one of the fundamental steps toward an effective immune response *in vivo*. The next step in our study was therefore to determine if DCs and Macrophages (M ϕ s) produce mediators such as cytokines in response to our vaccine candidate. We performed ELISA assays to measure pro-inflammatory cytokine expression (IL-6, IL-1 β , TNF- α , IL-10, IFN- γ , IFN- α and IL-12p40) after incubation of BMDCs and peritoneal M ϕ s with DGNP, free TE or DGNP/TE.

The ELISA analysis indicated that the levels of IL1- β , IL-12p40, IL-6 and TNF- α secreted by BMDCs (Fig. 7A–D) and M ϕ s (Fig. 7F–I) after stimulation with DGNP/TE were significantly higher than that produced by the stimulation of DGNP or free TE.

The BMDCs stimulated with free TE or DGNP/TE did not produce significantly more IL-10 than those stimulated with DGNP alone

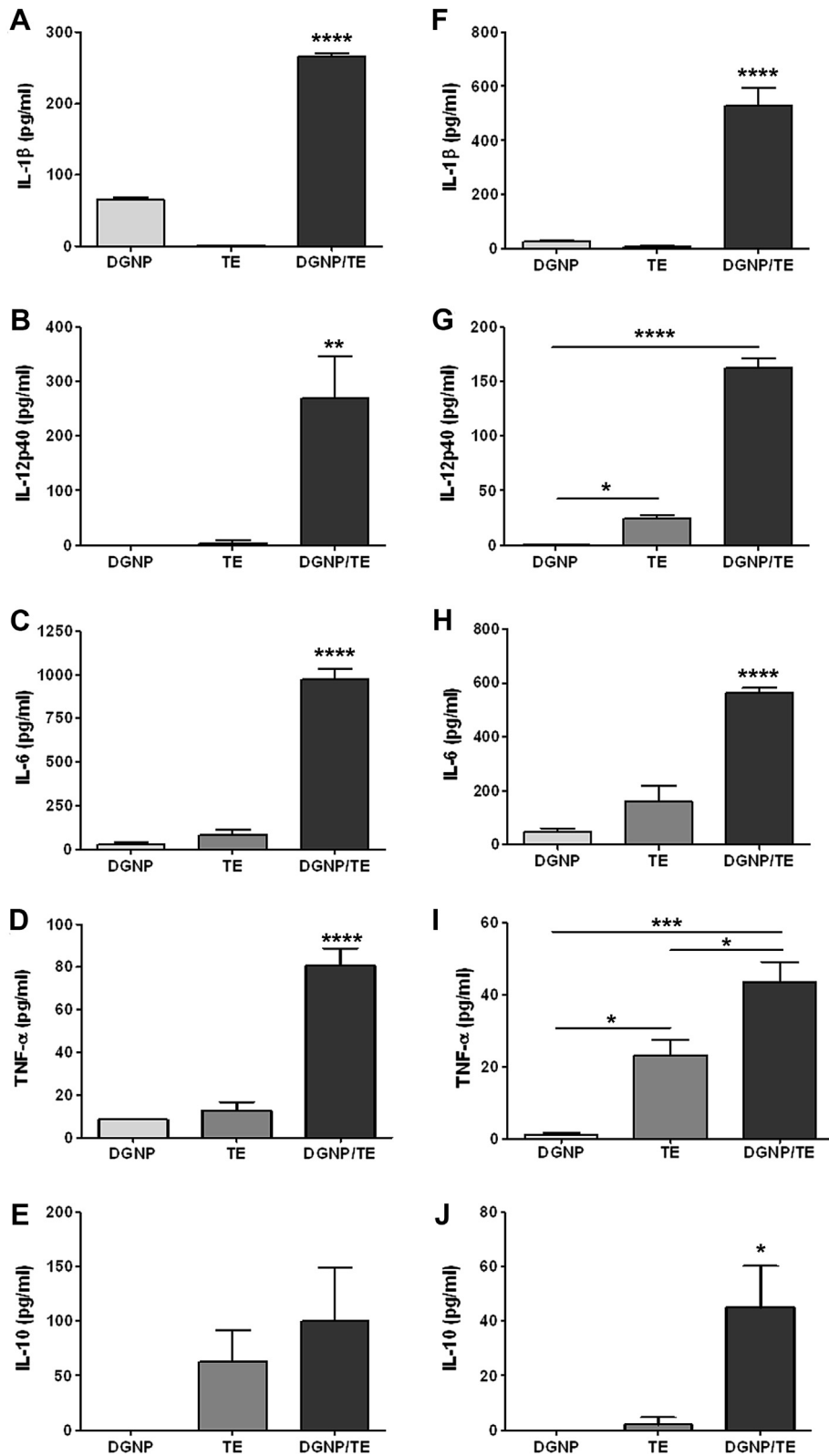


Fig. 7. Quantification by ELISA assay of cytokine secretion pattern of BMDCs (A–E) and M0s (F–J) treated with free or DGNP-encapsulated TE *in vitro*. The supernatants of APCs were collected and the concentrations of IL-1β (A, F), IL-12p40 (B, G), IL-6 (C, H), TNF-α (D, I) and IL-10 (E, J) were analyzed. These results are representative of at least three independent experiments. ****: $p < 0.0001$, ***: $p < 0.001$, **: $p < 0.01$, *: $p < 0.05$.

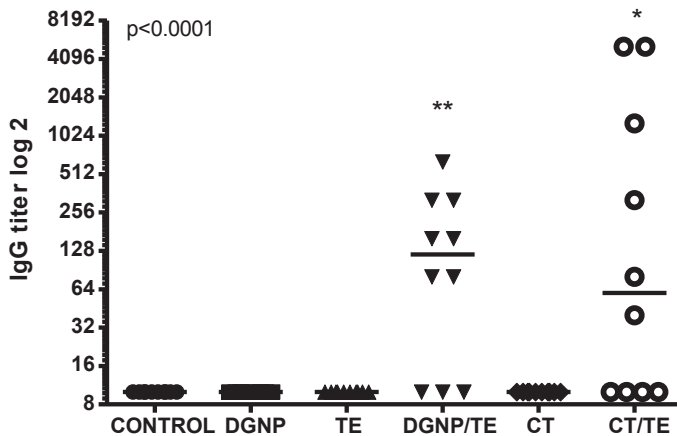


Fig. 8. Humoral response after vaccination. Detection by ELISA of specific anti-*T. gondii* IgG 15 days after the final immunization in serum from mice immunized by the nasal route with DGNP only, TE only or DGNP-formulated TE and with CT only or TE adjuvanted with CT. Serum samples from each mouse in each group were analyzed individually, with each dot representing a single mouse and bars showing the median. Data are representative of at least three independent experiments. *: $p < 0.05$, **: $p < 0.01$.

(Fig. 7E). However a statistically significant increase was obtained in MØs (Fig. 7J). No specific release of IFN- γ or IFN- α from any culture supernatant was observed (data not shown).

3.9. Intranasal delivery of DGNP/TE induces robust *Toxoplasma* specific humoral immune responses

Mice were vaccinated intra-nasally with DGNP, CT, free TE, CT/TE or DGNP/TE and ELISA analysis of specific IgG, IgG1 and IgG2a antibodies were performed on their sera. As shown in Fig. 8, higher levels of total IgG were detected only in the sera of mice immunized with CT/TE and DGNP/TE after the third immunization. In contrast, control mice or mice injected with free TE, TE alone or DGNP alone did not generate anti-*Toxoplasma* antibodies. To find out whether a Th1 and/or a Th2 humoral response was induced by DGNP/TE immunization, the level of specific IgG1 versus IgG2a sub-classes directed against TE were measured. The mixed IgG1/IgG2a response detected in the sera of mice immunized with DGNP/TE suggests that the specific immune response is Th1/Th2-biased (data not shown).

3.10. Intranasal delivery of DGNP/TE induces robust *Toxoplasma* specific cellular immune responses

Cell-mediated immune response is essential for the control of *T. gondii* and Th1 cytokines are critical for coordinating protective immunity against the parasite.

To determine whether nasal route vaccination with DGNP/TE could induce cellular immunity, Th1 cytokines (IFN- γ , IL-2, TNF- α), Th2 cytokines (IL-6, IL-4), Treg cytokine (IL-10) and Th17 cytokine (IL-17) were analyzed in the supernatant of TE-restimulated splenocytes and mesenteric lymph node cells from immunized mice.

After TE stimulation, only specific production of IFN- γ , TNF- α , IL6 and IL-17 was induced in splenocytes from the group of mice immunized with DGNP/TE (Fig. 9A, C, F, H). As expected, the number of IFN- γ -secreting splenocytes after TE stimulation detected in the ELISPOT wells was higher for mice immunized with DGNP/TE (Fig. 9B).

Spleen cells from mice immunized with free TE or DGNP/TE produced significantly more IL-2 (Fig. 9D) compared to those either

immunized or not with DGNP alone. However the specific secretion of IL-2 of spleen cells from mice immunized with DGNP/TE was not statistically different from that of spleen cells from mice immunized with free TE (Fig. 9D).

Anti-inflammatory cytokines (IL-10 and IL-4) production was not increased (Fig. 9E, G).

These results suggest that a mixed Th1/Th17 response was induced following immunization with DGNP/TE. The specific secretion of IFN- γ and IL-17 was probably due to CD4-specific T cells, as demonstrated with CD4-specific mAb during *in vitro* TE stimulation. In contrast, adding an anti-CD8 mAb to the cultures did not cause any significant reduction in the IFN- γ and IL-17 secretion. Mice immunized with DGNP/TE displayed a T CD4 cell response significantly higher than that elicited in the other groups (Fig. 9I–J).

3.11. DGNP/TE immunization protects against acute and chronic toxoplasmosis

In order to evaluate the protective effect of DGNP/TE vaccine against acute toxoplasmosis, vaccinated and control mice were challenged with a lethal dose of cysts (120 cysts) of the 76K strain of *T. gondii* 4 weeks after the last immunization. Their survival was monitored over 45 days. Within 12 days after infection, while DGNP/TE mice were totally protected, all mice of the others groups had succumbed (Fig. 10A).

To evaluate the contribution of the same DGNP/TE vaccine in the induction of a protective immune response against chronic toxoplasmosis, vaccinated mice were orally infected with 30 cysts (sub-lethal dose) of the 76K strain of *T. gondii*. CT/TE treated mice had significantly fewer cysts (901 cysts) than DGNP mice (1873 cysts) as well as CT mice (1816 cysts) ($p < 0.0001$). However no significant reduction was observed compared with control mice (1980 cysts) or free TE mice (1708 cysts) and DGNP/TE mice (611 cysts). DGNP/TE treated mice had significantly fewer cysts (611) than controls (1980), as well as compared with mice treated with DGNP only (1873 cysts) or free TE (1708 cysts) (DGNP/TE vs free TE cysts; $p < 0.0001$). The cyst reduction rate observed with DGNP/TE vaccination was 70% (Fig. 10B).

These results suggest that DGNP/TE vaccine reduces parasite growth and protects mice against long-term infection.

4. Discussion

The mucosal surface is the largest route through which pathogens enter the human body. To control the outbreak of mucosal infectious diseases, it is necessary to elicit both protective mucosal and systemic immunity. Mucosal vaccines have advantages over traditional injection vaccines in that they not only induce effective mucosal immune responses, but they also do not cause physical or psychological discomfort: in this regard, intranasal vaccines represent an attractive and valid alternative to conventional vaccines. To improve the efficiency of these vaccines, adjuvants or delivery systems are needed. So far many studies have shown the potential of nanoparticles to improve the immunogenicity of nasal vaccines. However little is known concerning their ability to deliver the antigens in the mucosa and how the immune system is elicited. In this study we propose a rational design concerning the use of porous DGNP nanoparticles as an antigen delivery system in airway mucosa to generate an innovative and efficient mucosal vaccine against *T. gondii*. *T. gondii* vaccine strategies usually use purified isolated antigens as protein or DNA-producing protein system. In this study, a total antigen extract of *T. gondii* (TE) has been produced to ensure samples to represent all the diversity and complexity of *T. gondii* antigens. This TE has been associated with DGNP nanoparticles to create vaccine formulations. DGNP are composed of a

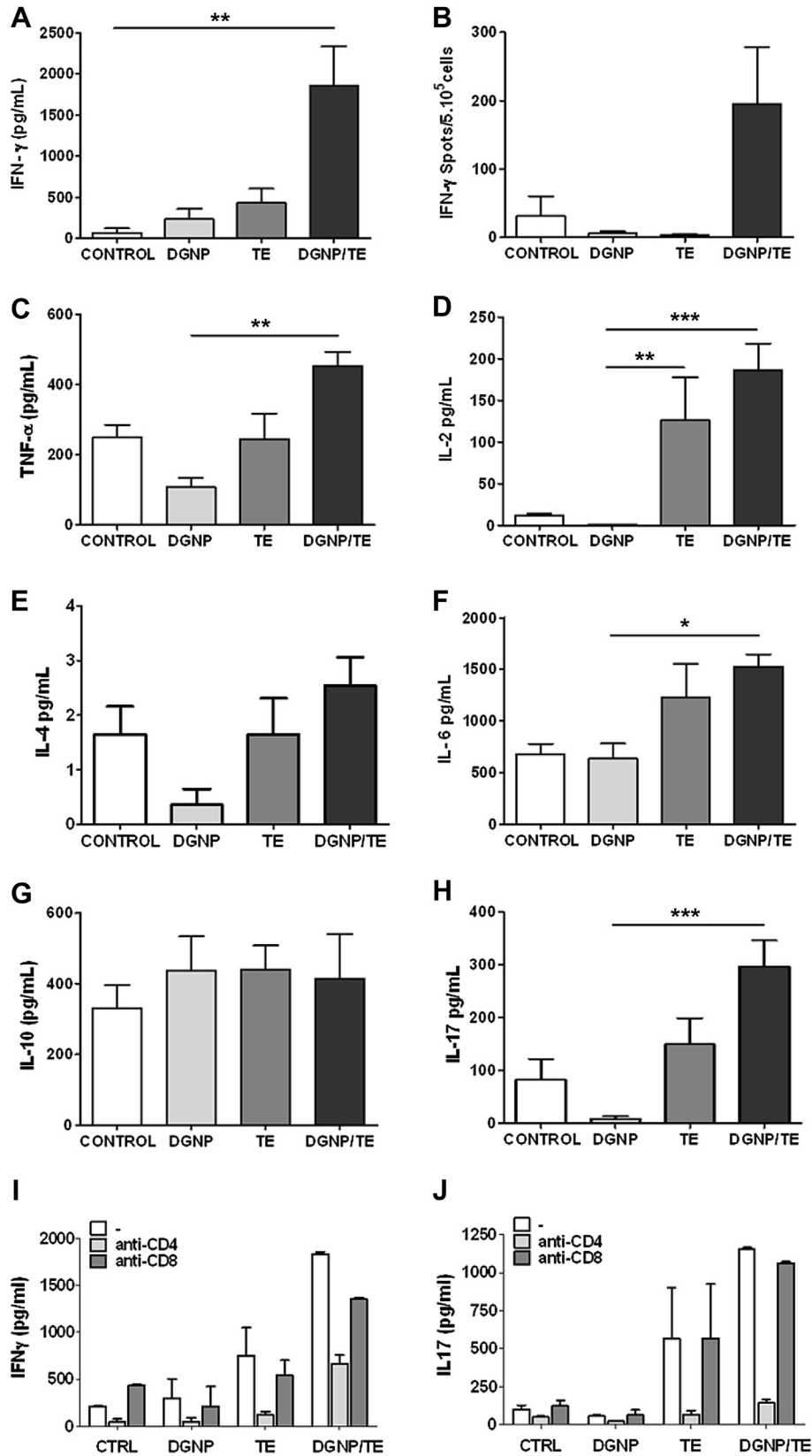


Fig. 9. Cellular response after vaccination. The CBA/J mice were immunized with DGNP, TE or DGNP/TE three times at 2-week intervals by the nasal route. Splenocytes were recovered 1 month after the final immunization and cultured with 10 μ g/mL TE. Splenocytes from six mice in each group were tested individually. Controls were untreated mice. Th1 cytokines (IFN- γ , TNF- α , IL-2) (A–D), Th2 cytokines (IL-6, IL-4) (E–F), Treg cytokines (IL-10) (G) and Th17 cytokines (IL-17) (H) were analyzed by Cytometric Bead Array Th1/Th2/Th17. (B) Intracellular IFN- γ was measured by Elispot analysis. Results are presented as number of IFN- γ -positive cells cultured with TE, minus number of IFN- γ -positive control cells. IFN- γ (I) and IL-17 (J) were measured in the absence or the presence of 20 μ g/mL of anti-CD4 or anti-CD8 mAb. Controls were untreated mice. *: $p < 0.05$, **: $p < 0.01$, ***: $p < 0.001$.

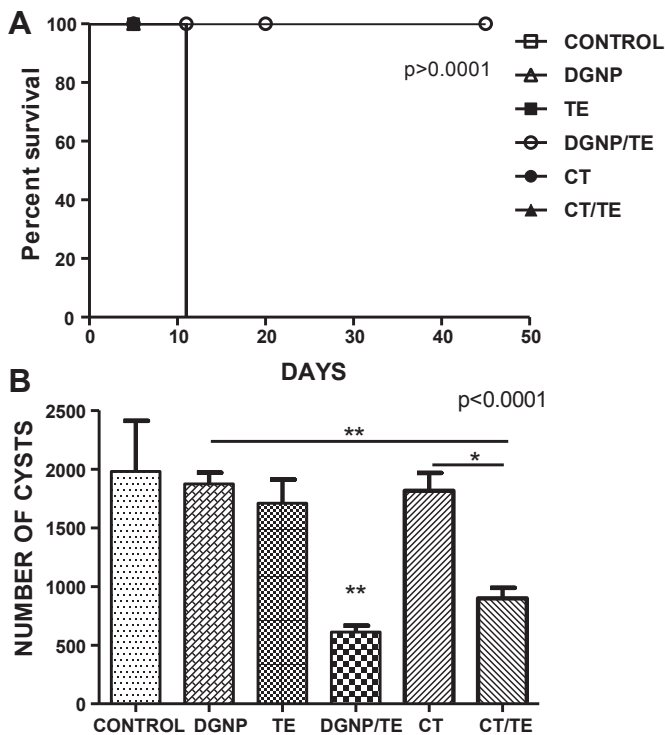


Fig. 10. Protection after vaccination. (A) Survival after oral infection of mice with 120 cysts of the 76K *T. gondii* strain. Data are expressed as percentage of cumulative survival during the experiment. The total number of tested animals in each group was $n = 7$, statistical analysis was performed using Chi Square Test. (B) Brain cyst load of CBA/J mice immunized by the nasal route with DGNP, CT, TE only, CT/TE, DGNP/TE, on days 0, 15 and 30 and orally infected with 30 cysts of 76K *T. gondii* strain. Brain cyst load was evaluated 1 month after challenge. Vaccination with CT/TE and even more with DGNP/TE significantly reduced the formation of brain cyst compared to control mice. Data are representative results of three independent experiments and are expressed as the means \pm SEM. *: $p < 0.05$, **: $p < 0.01$.

cationic maltodextrin matrix enclosing DPPG in their core as shown by zeta potential study [37]. Importantly, DPPG favors the cytoplasmic delivery of vectorized proteins/antigens [35]. The quality of antigens loading in the NP is mainly due to ionic interactions and is not modified by DPPG even if the amount of protein loaded in DGNP is lower than NP without lipid core [37]. DGNP appeared as a good candidate for antigen delivery in cells.

We first observed that DGNP nanoparticles are able to be loaded with large amounts of proteins in their core [38] without being saturated, so that the surface of the nanoparticles remains cationic. Furthermore, complex extracts of antigens with heterogeneous molecular weights can also be totally incorporated in a quantitative manner. It is interesting to note that at our knowledge this percentage of loading (100 μ g of proteins for 100 μ g of nanoparticles) has not been described earlier and is far higher than that observed with hollow silica mesoporous nanoparticles [38]. Electrophoresis study emphasized the stability of antigens/DGNP interactions. Indeed all TE components were associated to nanoparticles and long-term storage of formulations did not evidence any dissociation of TE from DGNP (unpublished data). We also demonstrated that, contrary to what was observed with free antigens, DGNP were also able to efficiently deliver the antigens into airway epithelial cells, macrophages and DCs. The presence of serum proteins decreased, but not abolished, the delivery of proteins into cells. It is known that serum proteins can decrease NP endocytosis, and the decrease of the endocytosis observed here could be related to a decrease of the NPs' zeta potential [39,40]. This delivery induced the activation of these cells *via* the NF- κ B pathway, through TLR2

and TLR4 signaling and the production of pro-inflammatory cytokines [41]. This suggests that the *Toxoplasma* extract TE contains factors including (though probably not exclusively) the GPI and HSP70 able to trigger the TLR2 and TLR4 signaling pathways [42,43]. Vaccine strategies are often dependent on subcutaneous or intra-muscular injection. Our strategy aim at eliciting an immune response triggering first the mucosal way, as natural infection would do. *In vivo*, vaccine was administered by the nasal route. Mice vaccinated with DGNP/TE developed a delayed humoral response and a protective and specific Th1/Th17 response. Only mice vaccinated with DGNP/TE survived acute toxoplasmosis while a significant decrease of brain cysts was observed in chronic toxoplasmosis.

5. Conclusion

The development of an efficient vaccine against *T. gondii* infection can only be done with innovative alternatives like nanoparticles-based approach combined with heterogeneous antigens of parasite. To nearest mimic natural infection, the mucosal route is used as administration site. DGNP nanoparticles are able to delivered total antigens extract to cells to elicit an humoral and a Th1/Th17 cellular immune response. Moreover, only mice vaccinated with our DGNP/antigens formulation survived to a lethal dose of parasites. This proof-of-concept results show an original and efficient strategy to vaccine against *T. gondii* infection. This clearly demonstrates the utility of DGNP nanoparticles as vaccine delivery system and confirm that the rational design of intranasal vaccines requires an in-depth understanding of the molecular mechanisms governing the activation of the innate and adaptive immune system.

Acknowledgments

All authors have given approval to the final version of the manuscript. Authors would like to thank Mike Howsam for corrections and proofreading, Sylvie Bigot, Bruno Héraud (University of Tours) and Nathalie Jouy, Emeline Machez, Meryem Tardivel, from the cytometry and cell imaging facilities of IFR114-IMPRT (University of Lille 2) for scientific discussions and technical assistance. This work was partially funded by the French A.N.R. (Agence Nationale de la Recherche) through Grant ANR-12-EMMA-0032-02 entitled "NanoToxo".

References

- [1] Pliaka V, Kyriakopoulou Z, Markoulatos P. Risks associated with the use of live-attenuated vaccine poliovirus strains and the strategies for control and eradication of paralytic poliomyelitis. *Expert Rev Vaccines* 2012;11:609–28.
- [2] Azmi F, Ahmad Fuaad AA, Skwarczynski M, Toth I. Recent progress in adjuvant discovery for peptide-based subunit vaccines. *Hum Vaccines Immunother* 2013;10.
- [3] van Riet E, Ainai A, Suzuki T, Kersten G, Hasegawa H. Combatting infectious diseases; nanotechnology as a platform for rational vaccine design. *Adv Drug Deliv Rev* 74, 2014;74:28–34.
- [4] Moon JJ, Suh H, Bershteyn A, Stephan MT, Liu H, Huang B, et al. Interbilayer-crosslinked multilamellar vesicles as synthetic vaccines for potent humoral and cellular immune responses. *Nat Mater* 2011;10:243–51.
- [5] De Koker S, Lambrecht BN, Willart MA, van Kooyk Y, Grooten J, Vervaeke C, et al. Designing polymeric particles for antigen delivery. *Chem Soc Rev* 2011;40:320–39.
- [6] Reddy ST, van der Vlies AJ, Simeoni E, Angeli V, Randolph GJ, O'Neil CP, et al. Exploiting lymphatic transport and complement activation in nanoparticle vaccines. *Nat Biotechnol* 2007;25:1159–64.
- [7] Kwon YJ, James E, Shastri N, Frechet JM. In vivo targeting of dendritic cells for activation of cellular immunity using vaccine carriers based on pH-responsive microparticles. *Proc Natl Acad Sci U S A* 2005;102:18264–8.
- [8] Kasturi SP, Skountzou I, Albrecht RA, Koutsouanos D, Hua T, Nakaya HI, et al. Programming the magnitude and persistence of antibody responses with innate immunity. *Nature* 2011;470:543–7.

- [9] Hill D, Dubey JP. *Toxoplasma gondii*: transmission, diagnosis and prevention. Clin Microbiol Infect 2002;8:634–40.
- [10] Joynton DHM, Wreghitt TG, editors. Toxoplasmosis: a comprehensive clinical guide. Cambridge University Press; 2001. p. 74.
- [11] Buxton D. Protozoan infections (*Toxoplasma gondii*, *Neospora caninum* and *Sarcocystis* spp.) in sheep and goats: recent advances. Veterinary Res 1998;29:289–310.
- [12] Frenkel JK. Pathophysiology of toxoplasmosis. Parasitol Today 1988;4:273–8.
- [13] Denkers EY, Gazzinelli RT. Regulation and function of T-cell mediated immunity during *Toxoplasma gondii* infection. Clin Microbiol Rev 1998;11:569–88.
- [14] Gazzinelli R, Hakim FT, Hieny S, Shearer GM, Sher A. Synergistic role of CD4⁺ and CD8⁺ T lymphocytes in IFN-gamma production and protective immunity induced by an attenuated *Toxoplasma gondii* vaccine. J Immunol 1991;146:286–92.
- [15] Gazzinelli R, Xu Y, Hieny S, Cheever A, Sher A. Simultaneous depletion of CD4⁺ and CD8⁺ T lymphocytes is required to reactivate chronic infection with *Toxoplasma gondii*. J Immunol 1992;149:175–80.
- [16] Suzuki Y, Orellana MA, Schreiber RD, Remington JS. Interferon- γ : the major mediator of resistance against *Toxoplasma gondii*. Science 1988;240:516–8.
- [17] Suzuki Y, Remington JS. Dual regulation of resistance against *Toxoplasma gondii* infection by Lyt-2⁺ and Lyt-1+, L3T4⁺ T cells in mice. J Immunol 1988;140:3943–6.
- [18] Shirahata T, Yamashita T, Ohta C, Goto H, Nakane A. CD8⁽⁺⁾ T lymphocytes are the major cell population involved in the early gamma interferon response and resistance to acute primary *Toxoplasma gondii* infection in mice. Microbiol Immunol 1994;38:789–96.
- [19] Khan IA, Ely KH, Kasper LH. Antigen-specific CD8(+) T cell clone protects against acute *Toxoplasma gondii* infection in mice. J Immunol 1994;152:1856–60.
- [20] Casciotti L, Ely KH, Williams ME, Khan IA. CD8⁺-T-cell immunity against *Toxoplasma gondii* can be induced but not maintained in mice lacking conventional CD4⁺ T cells. Infect Immun 2002;70:434–43.
- [21] Lycke N. Recent progress in mucosal vaccine development: potential and limitations. Nat Rev Immunol 2012;12:592–605.
- [22] Neutra MR, Kozlowski PA. Mucosal vaccines: the promise and the challenge. Nat Rev Immunol 2006;6:148–58.
- [23] Bulow R, Boothroyd JC. Protection of mice from fatal *Toxoplasma gondii* infection by immunization with p30 antigen in liposomes. J Immunol 1991;147:3496–500.
- [24] Hedhli D, Dimier-Poisson I, Judge JW, Rosenberg B, M ev elec MN. Protective immunity against *Toxoplasma* challenge in mice by coadministration of *T. gondii* antigens and *Eimeria* profilin-like protein as an adjuvant. Vaccine 2009;27:2274–81.
- [25] Grover HS, Blanchard N, Gonzalez F, Chan S, Robey EA, Shastri N. The *Toxoplasma gondii* peptide AS15 elicits CD4 T cells that can control parasite burden. Infect Immun 2012;80:3279–88.
- [26] Azegami T, Yuki Y, Kiyono H. Challenges in mucosal vaccines for the control of infectious diseases. Int Immunol 2014;26:517–28.
- [27] Debard N, Buzoni-Gatel D, Bout D. Intranasal immunization with SAG1 protein of *Toxoplasma gondii* in association with cholera toxin dramatically reduces development of cerebral cysts after oral infection. Infect Immun 1996;64:2158–66.
- [28] Lycke N, Holmgren J. Strong adjuvant properties of cholera toxin on gut mucosal immune responses to orally presented antigens. Immunology 1986;59:301–8.
- [29] Elson CO, Ealding W. Generalized systemic and mucosal immunity in mice after mucosal stimulation with cholera toxin. J Immunol 1984;132:2736–41.
- [30] Klippstein R, Pozo D. Nanotechnology-based manipulation of dendritic cells for enhanced immunotherapy strategies. Nanomed Nanotechnol Biol Med 2010;6:523–9.
- [31] Okamoto S, Matsuura M, Akagi T, Akashi M, Tanimoto T, Ishikawa T, et al. Poly(γ -glutamic acid) nano-particles combined with mucosal influenza virus hemagglutinin vaccine protects against influenza virus infection in mice. Vaccine 2009;27:5896–905.
- [32] Caputo A, Castaldello A, Brocca-Cofano E, Voltan R, Bortolazzi F, Altavilla G, et al. Induction of humoral and enhanced cellular immune responses by novel core-shell nanosphere- and microsphere-based vaccine formulations following systemic and mucosal administration. Vaccine 2009;27:3605–15.
- [33] Debin A, Kravtsov R, Santiago JV, Cazales L, Sperandio S, Melber K, et al. Intranasal immunization with recombinant antigens associated with new cationic particles induces strong mucosal as well as systemic antibody and CTL responses. Vaccine 2002;20:2752–63.
- [34] Dombu CY, Betbeder D. Airway delivery of peptides and proteins using nanoparticles. Biomaterials 2013;34:516–25.
- [35] Dombu C, Carpentier R, Betbeder D. Influence of surface charge and inner composition of nanoparticles on intracellular delivery of proteins in airway epithelial cells. Biomaterials 2012 Dec;33(35):9117–26. <http://dx.doi.org/10.1016/j.biomaterials.2012.08.064>.
- [36] Ismael AB, Sekkai D, Collin C, Bout D, Mevelec MN. The MIC3 gene of *Toxoplasma gondii* is a novel potent vaccine candidate against toxoplasmosis. Infect Immun 2003;71:6222–8.
- [37] Paillard A, Passirani C, Saulnier P, Kroubi M, Garcion E, Benoit JP, et al. Positively-charged, porous, polysaccharide nanoparticles loaded with anionic molecules behave as 'stealth' cationic nanocarriers. Pharm Res 2010;27:126–33.
- [38] Mahony D, Cavallaro AS, Mody KT, Xiong L, Mahony TJ, Qiao SZ, et al. In vivo delivery of bovine viral diarrhoea virus, E2 protein using hollow mesoporous silica nanoparticles. Nanoscale 2014;6:6617–26.
- [39] Smith PJ, Giroud M, Wiggins HL, Gower F, Thorley JA, Stolpe B, et al. Cellular entry of nanoparticles via serum sensitive clathrin-mediated endocytosis, and plasma membrane permeabilization. Int J Nanomed 2012;7:2045–55.
- [40] Merhi M, Dombu CY, Briant A, Chang J, Platel A, Le Curieux F, et al. Study of serum interaction with a cationic nanoparticle: Implications for in vitro endocytosis, cytotoxicity and genotoxicity. Int J Pharm 2012;423:37–44.
- [41] Iwasaki A, Medzhitov R. Toll-like receptor control of the adaptive immune responses. Nat Immunol 2004;5:987–95.
- [42] Debierre-Grockieo F, Campos MA, Azzouz N, Schmidt J, Bieker U, Resende MG, et al. Activation of TLR2 and TLR4 by glycosylphosphatidylinositols derived from *Toxoplasma gondii*. J Immunol 2007;179:1129–37.
- [43] Aosai F, Rodriguez Pena MS, Mun HS, Fang H, Mitsunaga T, Norose K, et al. *Toxoplasma gondii*-derived heat shock protein 70 stimulates maturation of murine bone marrow-derived dendritic cells via Toll-like receptor 4. Cell Stress Chaperones 2006;11:13–22.